A Simulator Study Comparing Characteristics of Manual and Automated Driving During Lane Changes of Long Combination Vehicles

Peter Nilsson, Leo Laine, and Bengt Jacobson

***Abstract*— This paper presents a back-to-back performance comparison of lane-change maneuvers using two automated driving approaches and manual driving. The lane changes were conducted in a moving-base truck driving simulator using an A-double long combination vehicle. One of the automated driving approaches was based on driver model control and the other used optimization-based control. The comparison addresses lane change and braking, both initiation and execution, from the perspective of driver behavior and defined characteristic variables. We also discuss combined braking and steering behavior using a moderately safety-critical lane-change scenario. The purpose of this paper is to improve driving automation in early development by comparing and learning from professional truck drivers to enable higher driver acceptance.**

***Index Terms*— Automated highway vehicle, heavy-duty vehicle, lane change, driving simulator.**

I. Introduction

FOR about three decades, both academia and the industry have increasingly moved towards self-driving automation technology. These efforts have recently been accelerated thanks to increased computing capacity, which enables extensive data processing from vehicle environment sensors. Further, society and legislation are increasing demands for safe and efficient transports [1]. Although the public's main interest in self-driving automation technology primarily targets passenger cars, several automation research programmes have been initiated that also include heavy vehicles [2]–[4]. Moreover, as [5] points out, the primary motivation for automating vehicle driving differs between passenger cars and heavy vehicles. Self-driving passenger cars are mainly motivated by concerns about mobility, traffic safety, and freeing time for the driver. In most cases this requires a high level of automation, level 4 according to SAE J3016 [6], to such degree that the driver is not expected to be the fall-back solution in a sudden critical event. For commercial heavy vehicles, driving automation is instead mainly fuelled by productivity[1] and traffic safety concerns, which in some cases could potentially be met with lower levels of automation as long as productivity is improved. In addition to the differences in motivation, another concern that needs to be addressed in automating commercial heavy vehicles is their limited lateral stability even in quite normal driving conditions. For example, the rollover threshold in lateral acceleration can be as low as 3 $\mathrm{m\,s^{-2}}$ compared with a standard passenger car, which has no rollover threshold at all.

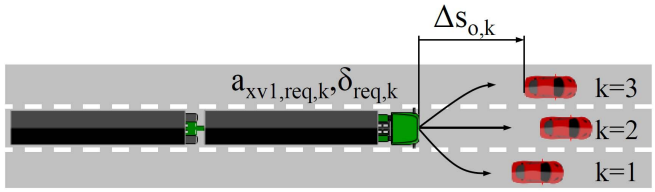

Fig. 1. Schematic representation of the A-double combination and an illustration of trajectories created in the traffic predictions including predicted actuation requests for current and adjacent lanes used in A1 [9].

An interesting starting point considering future heavy goods transports would be to combine, highly productive transport solutions with driving automation. This would further improve productivity, traffic safety and uptime. One example of highly productive long-haul road transports is long combination vehicles (LCVs), such as illustrated in Fig. 1. These are road transport vehicles whose length and weight dimensions fall outside that permitted in conventional European road regulations. Typically LCVs include at least two articulated joints and their length generally varies between 25.25 m and 34 m. The weight and/or volume of transported goods with LCVs is increased with a factor 1.5-2 compared to a conventional tractor semi-trailer combination. However, using LCVs can further amplify lateral motions in high speed manoeuvres such as lane changes compared to conventional vehicle combinations. Typical performance characteristics are rearward amplification of the lateral acceleration between the first and last vehicle units and lateral off-tracking between the first and last axles in the vehicle combination [7]. For example, during

Manuscript received June 8, 2016; revised October 25, 2016 and January 9, 2017; accepted January 14, 2017. Date of publication March 14, 2017; date of current version August 28, 2017. This work was supported in part by the Swedish National Research Programme FFI and in part by the Swedish Excellence Centre Virtual Prototyping and Assessment by Simulation (ViP) through the Swedish Automotive Industry and the Swedish Research Foundation Vinnova. The Associate Editor for this paper was J. Ploeg.

P. Nilsson and L. Laine are with the Department of Chassis Strategies and Vehicle Analysis, Volvo Group Trucks Technology, SE-405 08 Gothenburg, Sweden (e-mail: peter.q.nilsson@volvo.com; leo.laine@volvo.com).

B. Jacobson is with the Vehicle Dynamics Group, Division of Vehicle Engineering and Autonomous Systems, Department of Applied Mechanics, Chalmers University of Technology, SE-412 96 Gothenburg, Sweden (e-mail: bengt.jacobson@chalmers.se).

Color versions of one or more of the figures in this paper are available online at http://ieeexplore.ieee.org.

Digital Object Identifier 10.1109/TITS.2017.2664890

[1] Vehicle productivity can be defined as the difference between revenues and fixed and variable costs summed over the number of transport missions.

an LCV lane-change manoeuvre at 80 km h^{-1} the rearward amplification and the lateral off-tracking can be as high as 2 and 1 m, respectively. The corresponding values for a tractor semi-trailer combination are typically 1 and 0.2 m.

The assumed typical road usage of LCVs is one-way multiple lane roads. Driving is mainly expected to consist of in-lane cruising and more rarely manoeuvres such as lane changes, roadway departures, entrances, and overtaking. Based on expected road usage, the fundamental driving automation of LCVs is foreseen to include vehicle in-lane cruising and lane-change functionalities. In the case that there is a human occupant in the cabin during the transport mission, human comfort and driver/operator acceptance will add constraints to driving automation. The Safe Corridor Project [8] developed two approaches for introducing the necessary driving automation for LCVs. The implementation of the approaches can be categorised as conditional automation, automation level 3 [6]. The first approach is based on driver behaviour modelling [9] and the second uses non-linear model predictive control [10]; the performance of vehicle dynamics was compared in [11]. The approaches are further described in Section II-B.

One way of testing the developed driving automation is through physical vehicle testing. The drawback to this is that vehicle environment sensors need to be in place from the start and surrounding physical traffic needs to be controlled and included in the test scenarios. To avoid these problems, we chose a high-fidelity moving-base truck driving simulator instead. Driving simulators offer great control and reproducibility, but may have limited physical, perceptual, and behavioural fidelity [12]. Previously, driving simulator studies were mainly used to focus on the interaction between the driver and specific assistance functions, automation levels 0-2. More recently, there has been a new interest in using driving simulators to develop and evaluate automation level 3 and higher. For example, in [13] driving simulator studies were used for the development of highway driving automation level 3. In [14] simulator studies were conducted to assure driver acceptance of automation level 4. However, to the knowledge of the authors, no back-to-back performance comparison of highway driving automation level 3 and manual driving during lane changes has ever been conducted in a simulator study.

The main contributions of this article are: a back-to-back comparison of defined characteristic variables from automated driving level 3 for a commercial heavy vehicle and manual driving. The comparison focuses on lane changes and braking and their initiation and execution, in part from a driver behaviour perspective. It also discusses combined braking and steering based on observations from manual driving. The purpose is to improve driving automation in early development by comparing and learning from professional truck drivers, as well as to enable higher driver acceptance.

The remainder of the paper is structured as follows: Section II presents definitions of scenarios and the basis of driver behaviour for lane changes and braking. It also describes the principles of the automated driving approaches and the simulator experiment. Section III introduces the characteristic variables and combined braking and steering, while Section IV presents the results from observed data. Section V concludes with remarks on human perception and potential areas for future research.

II. Method

A. Driver Behaviour-Based Analysis

To objectively compare the manual and automated driving, we define characteristic variables for conducting lane changes in combination with human optical perceptual abilities. Therefore, we begin with a short review of driver behaviour literature considering lane changes, braking, and their initiation and execution. Firstly, a human driver's optical perceptual abilities are defined by the optical angle - the angular projection of an object [15]. When considering small angles, the optical projection of a lead vehicle θ_{lead}, can be approximated according to (1), where w is the width of the lead vehicle and Δs_{lead} is the difference in distance between the subject and the lead vehicle. The expansion rate of the optical angle $\dot{\theta}_{\text{lead}}$ can be calculated as (2), where Δv_{lead} is the difference in velocity between the subject and the lead vehicle. The quotient between the optical angle and the angular expansion rate τ_{lead} (3) is often cited as an example of an optical invariant, since it uniquely specifies time-to-collision independent of changes in the object size [16].

$$\theta_{\text{lead}} = \frac{w}{\Delta s_{\text{lead}}} \tag{1}$$

$$\dot{\theta}_{\text{lead}} = \frac{-w \cdot \Delta v_{\text{lead}}}{\Delta s_{\text{lead}}^2} \tag{2}$$

$$\tau_{\text{lead}} = \frac{\theta_{\text{lead}}}{\dot{\theta}_{\text{lead}}} \tag{3}$$

The motivation for lane-change initiation is often very complex to characterise, as the decision in general depends on the current traffic situation as well as a number of driver objectives including short-term and long-term aims. Based on microscopic traffic simulation, Gipps [17], proposed a structure to associate which decisions a driver must make before changing lanes. One of the main motivating factors is urgency, which is modelled through the drivers' instantaneous gap acceptance and predicted deceleration. A lane change is not initiated if predicted deceleration exceeded a certain value. Also, [18] shows that the feasibility of a lane change is evaluated using an acceptable deceleration level, which depends on the urgency of the manoeuvre. Study [19] defines a structured way of analysing the minimum safety spacing for lane changes. It shows that the relative speed between the subject vehicle and the lead vehicle in the target lane is of great importance for the minimum spacing requirement for a feasible lane change. If the magnitude of relative velocity is high, i.e. the vehicle in the target lane is moving faster than the subject vehicle, the minimum safety spacing becomes small.

Drivers' steering behaviour in lane-change execution, has been investigated in [20]. The results propose that visual feedback be used to adjust the direction resulting from a previous steering action in such a way that safety margins are controlled. Land and Lee [21] studied drivers' steering using visual heuristics and the connection between gaze and steering

wheel angle. Later, in [22], observations of lane changes supported the findings by Land and Lee, and formed the basis of a steering model proposed by Salvucci and Gray [23] involving two visual points. In this paper, the Salvucci and Gray's model is used in one of the automated approaches.

The task of braking, including initiation and execution, has been extensively studied in literature. According to [24] and [25], the ratio of the optical angle and the expansion rate is hypothesised to be an important stimulus for braking initiation. A model was developed in [25], that uses an inverse time-to-collision threshold that decreases linearly with speed to create a forward collision warning system. Lee [15] was one of the first to describe how braking execution can be solved using visual information. Lee proposed that braking performance can be specified using the variable τ and its time derivative $\dot{\tau}$, here referred to as the $\dot{\tau}$-strategy. In a closing situation it was shown that the subject vehicle deceleration is adequate if $\dot{\tau} \geq$ -0.5. An alternative to the $\dot{\tau}$-strategy, Smith et al. [26] propose that the optical angle and expansion rate are independent optical primitives and that braking could be controlled by weighting these to sources. Additional support for the individual use of optical angle and expansion rate was reported by Sun and Frost [27]. In this paper, one of the automated approaches uses the $\dot{\tau}$-strategy for braking.

B. Automated Driving Principles

Two automated driving approaches were evaluated in the experiments. The first is based on simulations using a driver model and the second is optimisation-based control, referred to as *A1* and *A2*. Each approach consists of an upper-level and a lower-level controller. The upper-level controller is placed in the traffic situation management and calculates requested longitudinal acceleration for the first vehicle unit $a_{x,1,\mathrm{req}}$ and front-wheel steering-angle actuation δ_{req} depending on the current traffic scenario. The lower-level controller is placed in the vehicle motion management and uses control allocation to coordinate the requested propulsion, braking and steering actuation [28]. The control allocation weighting matrix for actuator usage, e.g. braking in-between axles, is adapted to commercial heavy vehicles by using the actual normal force distribution in the weighting matrix [29].

Both automated driving approaches are implemented as individual driver support functions for automated driving including in-lane keeping and lane-change manoeuvres. As defined in the SAE standard J3016 [6], the functions can be categorised as conditional automation, automation level 3.

For both approaches, the driver is responsible for turning on and off the automated driving function and the ordering of lane-change manoeuvres during driving. The automated function is turned on and off using the switch that is normally used for the adaptive cruise control function. The driver communicates his lane change orders using the turn indicator. After such an order, and when each approach had found a feasible trajectory and been processed in the decision making, the automated lane change was started. To promote comfortable driving and avoid starting a lane change manoeuvre using a feasible trajectory with a small lead vehicle time gap (which possibly could lead to a high deceleration), the A1 approach includes a logic in the decision making stating that lane change start is only permitted when the time gap is greater than 2 s with respect to adjacent lead vehicle and less than −2 s with respect to adjacent lag vehicle. A negative time-gap means that the front of the lag vehicle are positioned behind the back of the subject-vehicle's rearmost trailer. For A2, no such logic is used in the decision making. Here, a time delay between lane-change order and lane-change start is enforced by the chosen methodology. The motivation behind this delay was to introduce the change of reference to the optimisation in a controlled manner. A sudden change of reference may temporarily lead to highly suboptimal control.

1) Driver Model Control - A1: In the *A1* approach, the predicted requested actuations are calculated using longitudinal and lateral driver models for manoeuvring in the current and adjacent left and right lanes of the LCV [9]. The predicted requested longitudinal accelerations $a_{\mathrm{xv1,req},k}$, where $k = 1, 2$ and 3 represent the current and adjacent lanes, are calculated as

$$a_{\mathrm{xv1,req},k} = (1 + \dot{\tau}_{\mathrm{m}}) \cdot \frac{\Delta v_{\mathrm{o},k}^2}{\left(\Delta s_{\mathrm{o},k} - v_{\mathrm{xv1}} \cdot \mathrm{TG}_{\mathrm{o,req}}\right)} \tag{4}$$

where $\dot{\tau}_{\mathrm{m}}$ is a constant parameter, $\Delta v_{\mathrm{o},k}$ is the relative speed between the subject-vehicle first-unit and the associated lead vehicle, $\Delta s_{\mathrm{o},k}$ is the relative distance between the front of the subject-vehicle and the associated lead vehicle, v_{xv1} is the subject-vehicle first-unit longitudinal speed, and $\mathrm{TG}_{\mathrm{o,req}}$ is the requested time gap to the associated lead vehicle. The initiation of braking and propulsion is based on margin values of the lead vehicle time gap and the optical expansion rate. Braking is initiated when the time gap is less than 2 s or the optical expansion rate larger than $0.2^\circ\,\mathrm{s}^{-1}$. In addition, if the requested jerk is larger than the jerk $j_{\mathrm{xv1,lim},k}$ (5), the acceleration is ramped up to its requested minimum value. The parameters $\underline{j}_{\mathrm{x}}$ and $\overline{j}_{\mathrm{x}}$ are the lower and upper limits of the jerk, and $\underline{a}_x$ is the lower limit of truck longitudinal acceleration. The longitudinal driver model is not designed for traffic situations where the lead vehicle is closer than the requested time gap e.g. a lead vehicle cut-in situation.

$$j_{\mathrm{xv1,lim},k} = \underline{j}_{\mathrm{x}} + \left(\overline{j}_{\mathrm{x}} - \underline{j}_{\mathrm{x}}\right) \cdot \frac{a_{\mathrm{xv1,req},k}}{\underline{a}_x} \tag{5}$$

The driver's predicted requested steering actuations are modelled with a two-point visual model [23] formulated as

$$\dot{\delta}_{\mathrm{req},k} = k_{\mathrm{f}} \cdot \dot{\theta}_{\mathrm{f},k} + k_{\mathrm{n}} \cdot \dot{\theta}_{\mathrm{n},k} + k_{\mathrm{I}} \cdot \theta_{\mathrm{n},k} \tag{6}$$

where $\dot{\delta}_{\mathrm{req},k}$ is the time derivative of the requested steering wheel angle, $\theta_{\mathrm{n},k}$ is the perceived angle to a near-point, and $\dot{\theta}_{\mathrm{f},k}$ and $\dot{\theta}_{\mathrm{n},k}$ are the angular velocities of the perceived angles to a far and near-point, respectively. Traffic situation predictions are carried out to verify the feasibility of the vehicle motion imposed by the requested actuations. The feasibility is verified in relation to kinematic and dynamic constraints including longitudinal (for maintaining the lateral grip margin) and lateral accelerations (for avoiding vehicle roll-over) (8)-(10), distance to lane boundaries (for avoiding

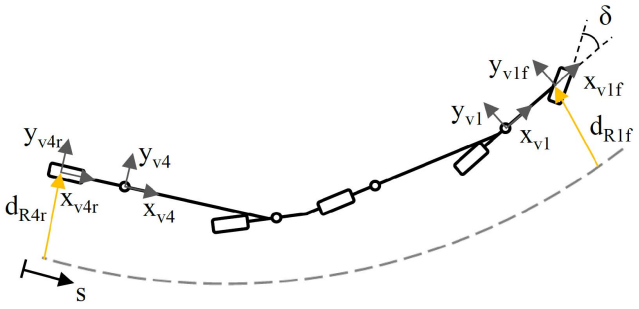

Fig. 2. Illustration of used reference frames in the A1 and A2 approaches.

driving off the road) (11)-(12) and distance to surrounding vehicles (for avoiding collisions) (13).

$$\underline{v}_x \leq v_{\mathrm{xv1},k}(t) \leq \overline{v}_x \tag{7}$$
$$\underline{a}_x \leq a_{\mathrm{xv1},k}(t) \leq \overline{a}_x \tag{8}$$
$$-\overline{a}_y \leq a_{\mathrm{yv1f},k}(t) \leq \overline{a}_y \tag{9}$$
$$-\overline{a}_y \leq a_{\mathrm{yv4r},k}(t) \leq \overline{a}_y \tag{10}$$
$$\underline{d} \leq d_{\mathrm{R1f},k}(t) \leq \overline{d} \tag{11}$$
$$\underline{d} \leq d_{\mathrm{R4r},k}(t) \leq \overline{d} \tag{12}$$
$$\underline{\Delta s}_{o,k} \leq \Delta s_{\mathrm{o},k}(t) \quad k = 1,2,3 \tag{13}$$

where a_{xv1} is the longitudinal acceleration of the first unit centre of gravity. a_{yv1f} and a_{yv4r} are the lateral accelerations of the first unit first axle and the fourth unit last axle, respectively. d_{R1f} and d_{R4r} are the lateral distances offset along the road of the first unit first axle and fourth unit last axle, see Fig. 2.

The traffic predictions, see Fig. 1, are carried out as closed-loop simulations including the driver models and prediction models of the LCV [30] and the surrounding vehicles, assuming constant acceleration. The predictions are made using the forward Euler method with a step size of 0.05 s and a prediction time of 3.75 s. If any constraint is violated, the prediction is identified as infeasible and the associated driving manoeuvre (lane keeping, lane changing or abort lane changing) is not available in the decision making. For example, if the subject-vehicle is in a lane-change manoeuvre and the associated prediction suddenly becomes infeasible, the subject-vehicle tries to shift to an abort lane-change manoeuvre. If the prediction associated with the abort maneuvre is feasible the abort manoeuvre is initiated, else the subject-vehicle shift to emergency brake. How the predictions are combined with decision making is further explained in [9].

2) Optimisation-Based Control - A2: In the *A2* approach, the requested control actuation is calculated using a non-linear model predictive control (NMPC) technique [10]. A constrained optimal control problem (OCP) describing the desired motion of the LCV over a finite future horizon is formulated. The OCP is transcribed into a non-linear program using a multiple shooting prediction model integration technique. In this approach, requested actuation is calculated for manoeuvring either in the current or an adjacent lane of the LCV. The subscript k used in the A1 approach is therefore omitted. The infinite dimensional optimal control problem and its constraints are formulated as

$$\begin{aligned}\min_{\xi(\cdot),u(\cdot)} \int_{s=0}^{s_f} \Big(& K_{d_{\mathrm{R1f}}} \cdot \left(d_{\mathrm{R1f}} - d_{\mathrm{R1f,ref}}\right)^2 + K_{d_{\mathrm{R4r}}} \\ & \cdot \left(d_{\mathrm{R4r}} - d_{\mathrm{R4r,ref}}\right)^2 \\ & + K_{v_{\mathrm{xv1}}} \cdot \left(v_{\mathrm{xv1}} - v_{\mathrm{xv1,ref}}\right)^2 + K_{j_{\mathrm{xv1}}} \cdot \left(j_{\mathrm{xv1}}\right)^2 \\ & + K_{j_{\mathrm{yv1}}} \cdot \left(j_{\mathrm{yv1}}\right)^2 + K_{a_{\mathrm{xv1}}} \cdot \left(a_{\mathrm{xv1}}\right)^2 + K_{\dot{\delta}} \cdot \dot{\delta}^2 \\ & + \sum_{k=1}^{3} K_{\Delta s_{o,k}} \cdot \left(f_{\mathrm{dk}}\left(\Delta s_{o,k}, v_{\mathrm{xv1f}}\right)\right)^2 \Big) d\sigma \end{aligned} \tag{14}$$
$$\frac{d\xi}{ds} = f(s,\xi,u) \tag{15}$$
$$\underline{a}_x \leq a_{\mathrm{xv1}}(s) \leq \overline{a}_x \tag{16}$$
$$-\overline{a}_y \leq a_{\mathrm{yv1f}}(s) \leq \overline{a}_y \tag{17}$$
$$-\overline{a}_y \leq a_{\mathrm{yv4r}}(s) \leq \overline{a}_y \tag{18}$$
$$\underline{d} \leq d_{\mathrm{R1f}}(s) \leq \overline{d} \tag{19}$$
$$\underline{d} \leq d_{\mathrm{R4r}}(s) \leq \overline{d} \tag{20}$$
$$\underline{\delta} \leq \delta(s) \leq \overline{\delta} \tag{21}$$
$$\underline{\dot{\delta}} \leq \dot{\delta}(s) \leq \overline{\dot{\delta}} \tag{22}$$
$$\underline{\Delta s}_{o,k} \leq \Delta s_{o,k} \quad k = 1,2,3 \quad \forall s \in [0, s_f] \tag{23}$$

where the first two terms in the cost function can be related to a lane-change efficiency or tracking objective. The reference trajectories $d_{\mathrm{R1f,ref}}$ and $d_{\mathrm{R4r,ref}}$ are in case of in-lane cruising the lane centreline, and in case of a lane-change manoeuvre the analytical solution to a point-mass system minimizing the lateral jerk. The reference trajectory $v_{\mathrm{xv1,ref}}$ is based on heuristics that includes the speed limit, the lateral acceleration caused by road curvature and comfortable lead vehicle following. The variables j_{xv1} and j_{yv1} are the longitudinal and lateral jerk expressed relative to a local coordinate frame positioned in the centre of gravity of the first LCV unit. The $\dot{\delta}$ is the road wheel angle. These terms promote smooth and comfortable driving. The term $f_{\mathrm{dk}}(\Delta s_{o,k}, v_{\mathrm{xv1f}})$ is related to distance keeping, which can be related to safety. The balance between efficiency, comfort, and safety is weighted with following factors: $K_{d_{\mathrm{R1f}}}$, $K_{d_{\mathrm{R4r}}}$, $K_{v_{\mathrm{xv1}}}$, $K_{j_{\mathrm{xv1}}}$, $K_{j_{\mathrm{yv1}}}$, $K_{a_{\mathrm{xv1}}}$, $K_{\dot{\delta}}$ and $K_{\Delta s_{o,k}}$. The constraint (15) is the equations of motion where ξ is the state vector and is dependent on the position of the front axle along the road and the control input. Constraints (17) and (18) limit the lateral accelerations of two positions of the LCV to prevent vehicle roll-over. Constraint (16) informs the trajectory generator of the physical maximum longitudinal acceleration of the LCV. Constraints (19) and (20) require two positions of the LCV to stay inside the lane boundaries. Constraints (21) and (22) reflect the maximum steering wheel angle and its time derivative, respectively, reflecting physical actuation constraints. Finally, (23) restricts a trajectory that collides with that of one of the surrounding vehicles. The logic governing which surrounding vehicles to consider in the OCP is largely implemented in a pre-processing stage to the OCP solver. Constraint (23) is introduced for each vehicle and promote longitudinal distance-keeping.

Further details on the optimal control problem formulation are found in [10].

A simple finite-state machine is implemented to handle the decision making between lane-keeping and lane-changing manoeuvres. The spatial prediction horizon is discretised using 50 intervals with a step size of 2 m. The dynamic constraints are imposed with a multiple-shooting integration scheme using a fourth-order explicit Runge-Kutta update rule taking five intermediate integration steps in each discretisation interval of the OCP. The used horizon length is 100 m and the control frequency is 2 m^{-1}.

C. Simulator Experiments

1) Driving Simulator and Implementation: Data were collected in the high fidelity moving-base truck driving simulator (SIMIV) at the Swedish National Road and Transport Research Institute in Gothenburg, Sweden. The motion platform [31] has 8 degrees of freedom (DOF) divided between a sledge with 2 DOF in the lateral and longitudinal direction and a hexapod with the remaining 6 DOF, 3 rotations and 3 translational displacements. The limitations of the system in terms of translational acceleration are 5 $m\,s^{-2}$ in both the lateral and longitudinal directions. A visual system provides a 180° field of view and emulated rear-view mirrors using monitor screens. A high fidelity two-track simulation model of an A-double combination vehicle, developed at Volvo Group Truck Technology, was used to emulate vehicle dynamics in the simulator. The model includes detailed sub-models of the vehicle chassis, cab suspension, steering system, powertrain and brakes. The studied A-double combination consists of a 6x4 tractor unit followed by a three-axle semi-trailer, two-axle dolly and a three-axle semi-trailer unit. The total vehicle length equals 32 m and the total weight is set to 80 t. The performance of the vehicle model is validated against real-world measurements. To further improve the realism, the motion cues generated by the driving simulator are tuned with the help of professional test drivers. The automated driving functions described in Section II-B are hosted in a conventional desktop computer running the Linux kernel, standard Arch distribution. The algorithms are implemented with C++ and have no runtime dependencies towards each other. The simulator closed-loop control frequency is synchronised with the control intervals of the automated approaches. The A1 approach is triggered at a control rate of 40 Hz, whereas the A2 approach is triggered every 2 m travelled along the lane centre line. When driving at a speed of 72 $km\,h^{-1}$, this corresponds to a control rate of 10 Hz.

At the beginning of each event the surrounding traffic was set at five distinct vehicles. These could either be passenger cars or trucks and their distribution was changed between events. Each vehicle was individually regulated in two different modes, either speed control or time-gap control. The controllers were selected according to the scenario demands and the control mode often changed between the two available conditions. In speed-control mode, the vehicle travelled either at the truck speed plus 1 $km\,h^{-1}$ or 62 $km\,h^{-1}$, whichever value was lower. This allows the truck driver or the automated driving approach to set a desired gap to the lead vehicle while eventually catching up to the road speed limit. An overview of the simulation layout including the components discussed above is further explained in [32].

2) Participants: Eighteen subjects, 17 men and 1 woman, participated in the study. All participants held a Swedish driving licence for heavy vehicles and 15 were at the time or had previously been professional truck drivers. Their driving experience varied widely; 7 of them drove more than 50,000 km yearly (mean 110,000 km/year, SD = 45,000 km/year) and 11 drove less (mean 13,700 km/year, SD = 17,200 km/year). The ages of the participants ranged from 28 to 63 years (mean 46.3 yrs., SD = 10.5 yrs.).

3) Event Design: The simulator study consisted of four individual events. The events were composed of a series of connected traffic actions that aimed to analyse specific driver characteristics during the course of a lane-change manoeuvre. The individual events were characterised as; *gap A*, *gap B*, *critical A* and *critical B*, see Fig. 3. The gap A and B events were designed to study driver preferences regarding lane-change initiation and manoeuvring. The critical A event was designed to study combined brake and steering actions, whereas the critical B event was constructed to study driver preferences regarding brake initiation and manoeuvring. In the experiment design, the events were combined into specific driving sessions to enable a smooth operating scheme.

The gap A and B events were either carried out as two consecutive events in the case of manual driving, or as a single event followed by a critical event in the case of automated driving, see Fig. 4. The difference in the event implementation between manual and automated driving was introduced to divide the manual driving into firstly non-critical and secondly critical lane change manoeuvres. The hypothesis was that if the drivers were subjected to a critical event first, this could lead to unnecessary cautiousness in a subsequent gap event. Initially in events gap A and gap B, the lead vehicle was in speed control mode, whereas all other vehicles were in time-gap control mode. When the driver switched on the turn indicator to request a lane change, the surrounding vehicles in the adjacent right lane displaced to open a gap. The size of the targeted gap depended on the specific driving session. When the centre of the front axle of the LCV tractor passed into the target lane, a countdown time was set for 7.5 s. When the counter reached zero, the adjacent lead vehicle activated speed control mode and the adjacent lag vehicle adjusted its gap to a smaller value, decreasing its distance to the rear of the truck. Finally, the vehicles in the left lane were set to gap-control mode defined in such a way as to prevent the subject vehicle from returning to the original lane. The different stages of the gap A and B events are illustrated in Fig. 3.

At the start of a critical A or B event, the surrounding vehicles were defined in the same control modes as in the gap events. The surrounding traffic in the adjacent right lane was modelled to open up a gap when the driver switched on the right turn indicator. This action was performed in the same way as for the gap events. The two main differences between the two critical events were *i)* which of the lead vehicles braked and *ii)* when the lead vehicle braking was initiated.

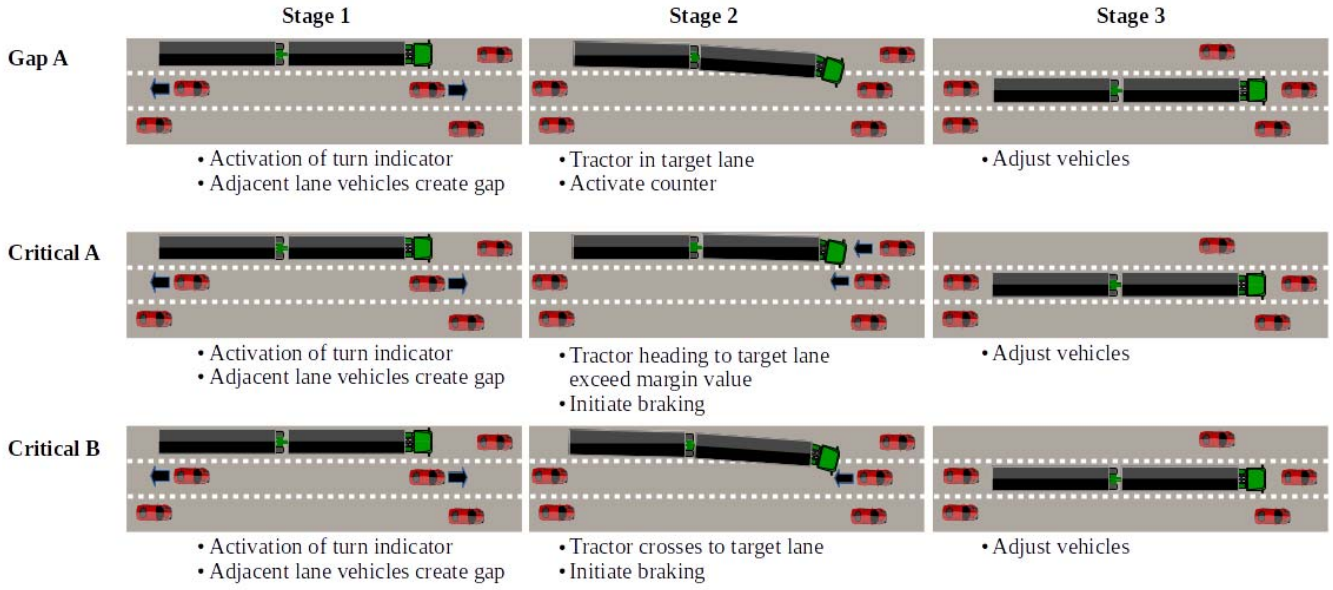

Fig. 3. Illustration of the different stages of events. Gap A (top row), critical A (middle row), critical B (bottom row). Gap B is identical to gap A with the exception that the lane change is initiated in the middle lane and finalised in the rightmost lane.

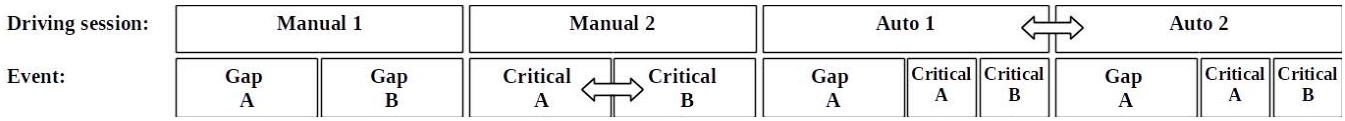

Fig. 4. Overview of experimental design with driving order from left to right. The arrows indicate that the order of the sessions and events were shifted randomly. For sessions auto 1 and 2, each driver drove either the critical A or the critical B event.

In the critical A event, both the lead vehicle in the current and adjacent target lane braked. The lead vehicle braking was initiated when the subject vehicle activated the turn indicator and the heading angle of the LCV tractor towards the target lane exceeded a margin value of 0.02 rad. The speed reduction was set to reach a pre-defined final speed of 40 km h^{-1} for the vehicle in the adjacent target lane and 35 km h^{-1} for the vehicle in the initial lane. In the critical B event, only the lead vehicle in the adjacent target right lane braked. The lead vehicle braking began when the subject vehicle had activated the turn indicator and the centre of the LCV front axle entered the target lane. The lead vehicle reference speed was set to 40 km h^{-1}. In all cases, the speed profiles of the braking lead vehicles were set to the sigmoid function to ensure smooth deceleration. Starting from the current speed of the vehicle, the speed reduction was actuated during a fixed time interval of 10 s and maintained for 3 s. Finally, the lead vehicle in the target lane activated speed-control mode and the vehicles in the left lane were set to gap-control mode defined in such way as to prevent the subject vehicle from returning to its original lane. The different stages of the two critical events are illustrated in Fig. 3. The critical A and B events were performed either one after the other in the case of manual driving, or following a gap A event, in the case of automated driving, see Fig. 4.

4) Experiment Design: The simulator study was organised in four distinct driving sessions: manual 1 and 2 and automated 1 and 2, which were separated by a short break in driving. Each session contained two events. Before starting the driving, the participants received both written and oral information about the simulator and the experiment and performed a driving training session. All sessions were driven on a one-way multiple lane road, consisting of sections of roads E20, E6 and R40, from intersection Anasmotet to Kallebacksbacken. The allowed speed limit is 70 km h^{-1}. The road used was modelled in the Knownroads project [33] using real-world measurements from GPS and map data as well as local road characteristics in terms of cross slope, incline and shorter vertical wave length data. Accurate height information on the surroundings and generic man-made structures were also added to the model. The automated driving was carried out using approaches A1 and A2; see Section II-B. Due to technical problems only 4 drivers used the A2 approach, whereas all drivers used the A1 approach. When possible, the order of the approaches was shifted randomly. An overview of the experimental design is provided in Fig. 4.

D. Definitions

Four driving events, further described in Section II-C.3, were developed to study highway driving of LCVs with focus on lane-change manoeuvres to the right, with and without adjacent lead vehicle braking. The driving was carried out on a three-lane one-way road with five surrounding vehicles, three of which were lead vehicles and two were lag vehicles as

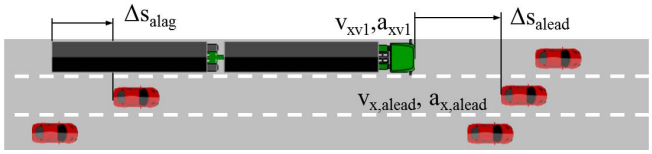

Fig. 5. Fundamental quantities in the general driving scenario.

illustrated in Fig. 5. In order to avoid ambiguity about which lead and lag vehicles are considered, a measure Δs related to the vehicles positioned in the adjacent right target lane is further referred to as either Δs_{alead} or Δs_{alag}.

Fundamental quantities in the driving events are subject-vehicle first-unit longitudinal speed v_{xv1}, adjacent lead vehicle speed $v_{\text{x,alead}}$, subject-vehicle first-unit longitudinal acceleration a_{xv1} and adjacent lead vehicle longitudinal acceleration $a_{\text{x,alead}}$. In addition, Δs_{alead} and Δs_{alag} are the adjacent lead and lag distance gaps, which are illustrated in Fig. 5. As regards lane-change manoeuvring, two definitions of the subject vehicle lane-change initiation (LCI), lane-change termination (LCT) and lane-change duration (LCD) are introduced. Provided that the turn indicator is activated, LCI1 is defined as when the heading angle of the tractor towards the target lane exceeds a margin value of 0.002 rad. LCI2 is defined as and when the inner front tyre passes the inside edge of the lane boundary, option D per SAE J2944 [34]. Similarly, LCT is defined as the occasion when the heading angle of the last vehicle unit towards the target lane is higher than a margin value of -0.002 rad for a time duration longer than 1 s, referred to as LCT1, and when all tyres are inside the lane boundary [34], referred to as LCT2. For braking, in the case that LCI1 has occurred, brake initiation (BI) of the subject and adjacent lead vehicles are defined as when the respective longitudinal accelerations are below a margin value of $-0.04\ \mathrm{m\,s^{-2}}$.

LCD is calculated as the time difference between LCT and LCI. Time gap (TG) is defined as the quotient between the distance gap and the subject vehicle speed (24)-(25). Time-to-collision (TTC) is defined as the distance gap divided by the difference in speeds per option B SAE J2944 [34], (26). Note that with this measure, the lead vehicle and subject vehicle speeds are assumed to remain constant throughout the manoeuvre. Rearward amplification of lateral acceleration (RA_{a_y}) is defined as the quotient between the peak magnitude lateral acceleration of the centres of gravity of last and first vehicle units (27).

$$\text{TG}_{\text{alead}} = \frac{\Delta s_{\text{alead}}}{v_{\text{xv1}}} \tag{24}$$

$$\text{TG}_{\text{alag}} = \frac{\Delta s_{\text{alag}}}{v_{\text{xv1}}} \tag{25}$$

$$\text{TTC}_{\text{alead}} = \frac{\Delta s_{\text{alead}}}{v_{\text{xv1}} - v_{\text{x,alead}}} = \frac{\Delta s_{\text{alead}}}{\Delta v_{\text{alead}}} \tag{26}$$

$$\text{RA}_{a_y} = \frac{a_{\text{yv4}}}{a_{\text{yv1}}} \tag{27}$$

III. Analysis

This section describes the analysis of lane change and braking. Characteristic variables connected to lane-change initiation and execution were studied using observed data from the gap A events. Brake initiation and execution were evaluated using the observed data from critical B events, and combined steering and braking was evaluated using the critical A events.

TABLE I
Summary of Characteristic Variables

Variable	Unit	Description
Lane-change initiation		
$\text{TG}_{\text{LCI1,alead}}$	s	Time gap to adjacent lead vehicle at LCI1
$\text{TG}_{\text{LCI1,alag}}$	s	Time gap to adjacent lag vehicle at LCI1
$\Delta v_{\text{LCI1,alead}}$	$\mathrm{m\,s^{-1}}$	Relative velocity to adjacent lead vehicle at LCI1
$\theta_{\text{LCI1,alead}}$	°	Optical angle at LCI1
$\dot{\theta}_{\text{LCI1,alead}}$	$^\circ\,\mathrm{s^{-1}}$	Rate of optical angle at LCI1
Lane-change execution		
LCD2	s	Lane-change duration based on LCI2 and LCT2
RA_{a_y}	-	Rearward amplification of lateral acceleration
$a_{\text{yv1,ext}}$	$\mathrm{m\,s^{-2}}$	Extremum of first unit lateral acceleration
$j_{\text{yv1,ext}}$	$\mathrm{m\,s^{-3}}$	Extremum of first unit lateral jerk
Brake initiation		
$\text{TG}_{\text{BI,alead}}$	s	Time gap to adjacent lead vehicle at BI
$\Delta v_{\text{BI,alead}}$	$\mathrm{m\,s^{-1}}$	Relative velocity to adjacent lead vehicle at BI
$\theta_{\text{BI,alead}}$	°	Optical angle at BI
$\dot{\theta}_{\text{BI,alead}}$	$^\circ\,\mathrm{s^{-1}}$	Rate of optical angle at BI
Brake execution		
$\tau^{-1}_{\text{max,alead}}$	$\mathrm{s^{-1}}$	Maximum inverse of TTC
$a_{\text{xv1,min}}$	$\mathrm{m\,s^{-2}}$	Minimum longitudinal acceleration
$j_{\text{xv1,min}}$	$\mathrm{m\,s^{-3}}$	Minimum longitudinal jerk
Combined braking and steering		
$d_{\text{R1f,BI}}$	m	Front axle lateral distance at BI

A. Characteristic Variables

Characteristic variables are defined to objectively evaluate the performance of automated and manual driving during lane-change manoeuvres. In respect of lane change and brake initiation, the expected safety margins were described as $\text{TG}_{\text{LCI1,alead}}$, $\text{TG}_{\text{LCI1,alag}}$, $\Delta v_{\text{LCI1,alead}}$, $\theta_{\text{LCI1,alead}}$ and $\dot{\theta}_{\text{LCI1,alead}}$; see the definitions in Sections II-A and II-D. For the lane-change execution, the safety margin and efficiency were characterised using RA_{a_y} and LCD2, respectively. Further, ride comfort was characterised by the extremum of the lateral acceleration and jerk of the first vehicle unit $a_{\text{yv1,ext}}$ and $j_{\text{yv1,ext}}$. For brake execution, the safety margin was represented by the maximum inverse of $\tau^{-1}_{\text{max,alead}}$ and ride comfort was characterised by the minimum longitudinal acceleration $a_{\text{xv1,min}}$ and jerk $j_{\text{xv1,min}}$ for the first vehicle unit. The characteristic variables are summarised in Table I.

B. Combined Braking and Steering

The combined braking and steering analysis focuses on the situation when the driver initialised a lane change in combination with the adjacent lead vehicle braking. In this situation, it is envisioned that the driver will either continue the lane change and combine braking and steering or abort the lane change by steering back to the initial lane and possibly braking. It is interesting from a driving automation perspective to examine accepted driving behaviour for LCVs and possible thresholds for initiating an abort manoeuvre. Prior to the experiment, the event was tuned in such a way that

TABLE II

TIME GAP WITH RESPECT TO ADJACENT LEAD VEHICLE AT LCI1 (GAP A)

	$TG_{LCI1,alead}$ (s)				
Mode	Mean	Median	Std	Max	Min
Manual	0.9	0.9	0.5	1.7	0.2
Auto 1	2.2	2.1	0.2	2.6	2.0
Auto 2	1.8	1.5	0.5	2.3	1.5

TABLE III

TIME GAP WITH RESPECT TO ADJACENT LAG VEHICLE AT LCI1 (GAP A)

	$TG_{LCI1,alag}$ (s)				
Mode	Mean	Median	Std	Max	Min
Manual	-0.8	-0.8	0.5	-0.1	-1.4
Auto 1	-1.9	-1.8	0.4	-1.7	-3.0
Auto 2	-2.3	-2.3	0.1	-2.3	-2.4

some subjects continued and some subjects aborted the lane change. The combined braking and steering was evaluated using longitudinal and lateral acceleration of the first vehicle unit and the lateral distance offset of the first unit first axle $d_{R1f,BI}$.

IV. RESULTS

The results presented are at most based on 17 drivers, since the data from one driver were corrupt. Further, we have excluded the results of drivers who maintained a vehicle speed below 45 km h^{-1} at lane change initiation in any of the critical events. As mentioned above in Section II-C.3, the targeted lead vehicle speed after braking in the critical events was either 40 km h^{-1} or 35 km h^{-1}. When the initial subject vehicle speed was below 45 km h^{-1} this resulted in very low levels of lead vehicle deceleration and the driving was not considered relevant for further analysis. Reviewing observed data showed that for the critical A and B events, 13 and 14 out of 17 manual drivers fulfilled the speed requirement.

A. Characteristic Variables

1) Lane-Change Manoeuvring (Gap A): Firstly, statistics of the $TG_{LCI1,alead}$ and $TG_{LCI1,alag}$ for lane-change initiation are given in Tables II-III. Considering manual driving, the mean values are 0.9 s and −0.8 s, respectively. As mentioned above in Section II-B, lane change initiation for automated approach A1 was only permitted when the time gaps to the adjacent lane vehicles were larger and smaller than ± 2.0 s, respectively. This behaviour is clearly reflected in the results and the mean values of $TG_{LCI1,alead}$ and $TG_{LCI1,alag}$ for the A1 approach are 2.2 s and −1.9 s, respectively. For the automated approach A2, the corresponding mean values are 1.8 s and −2.3 s. The targeted time gaps for A2, used in the cost function term related to distance keeping, are 2.0 s and −2.5 s.

Secondly, Fig. 6 shows the observed data on lane-change initiation for individual drivers. In the left panel of Fig. 6, the relationship between $TG_{LCI1,alead}$ and $\Delta v_{LCI1,alead}$ indicates that manual drivers who experience a large negative relative velocity also have a smaller time gap at LCI ($R^2 = 0.74$, $p = .0007$). When the relative velocity approaches zero,

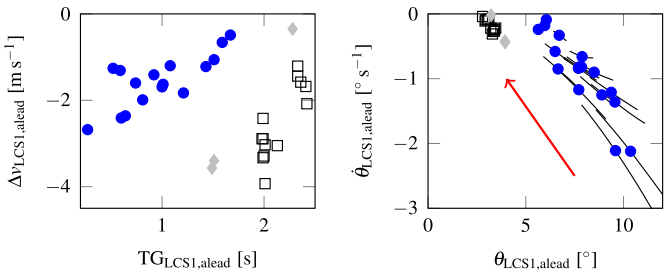

Fig. 6. Individual values of characteristic variables at lane-change initiation in the gap A events. The left panel shows $TG_{LCI1,alead}$ and Δv_{LCI1} and the right panel shows $\theta_{LCI1,alead}$ and $\dot{\theta}_{LCI1,alead}$. Manual driving is represented by solid blue circles. The solid black lines in the right panel represents individual trajectories one second before and after LCI1. The red arrow indicates time course. Automated driving A1 is represented by black squares and A2 is grey diamonds.

TABLE IV

REARWARD AMPLIFICATION OF LATERAL ACCELERATION (GAP A)

	RA_{a_y} (-)				
Mode	Mean	Median	Std	Max	Min
Manual	1.1	1.1	0.2	1.5	0.7
Auto 1	1.0	1.0	0.0	1.0	0.9
Auto 2	0.9	0.9	0.0	0.9	0.9

TABLE V

LANE-CHANGE DURATION LCD2 (GAP A)

	LCD2 (s)				
Mode	Mean	Median	Std	Max	Min
Manual	7.7	7.4	1.3	10.3	5.8
Auto 1	8.2	8.2	0.1	8.5	8.1
Auto 2	3.9	3.9	0.0	4.0	3.9

the time gap is approximately 2 s. These results correlate well with the minimum spacing requirement for a feasible lane change discussed in [19]. The impact of the relative speed difference was not considered in the automated driving approaches. Further, in the right panel of Fig. 6, the variables $\theta_{LCI1,alead}$ and $\dot{\theta}_{LCI1,alead}$ for the manual drivers suggest a linear relationship ($R^2 = -0.91$, $p = .0001$). This suggests that information regarding the possibilities for safe action in a lane-change situation are likewise found in the optical flow variables.

Table IV shows statistics of utilised RA_{a_y} in terms of lane-change execution and safety. Both the manual and automated driving suggest safe manoeuvring with the mean values 1.1 for manual driving and 1.0 and 0.9 for the A1 and A2 approaches. The theoretical maximum RA_{a_y} for the vehicle combination used is approximately 2. Driving efficiency characterised by LCD2 is given in Table V. The mean value of LCD2 for manual driving is 7.7 s, whereas the mean values for automated driving are 8.2 s and 3.9 s for the A1 and A2 approaches. The A2 approach is noticeably faster than both manual driving and the A1 approach.

The left panel of Fig. 7 shows observed mean values of $a_{yv1,ext}$ and LCD2, indicating that a fast lane change results in a high extremum of lateral acceleration, i.e. driving efficiency is in conflict with ride comfort. This result correlates well with

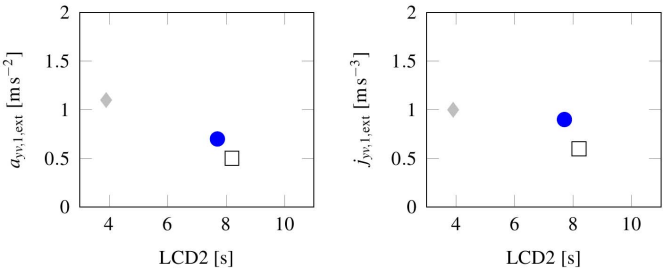

Fig. 7. Mean values of characteristic variables in the gap A events. The left panel shows LCD2 and $a_{yv1,ext}$, and the right panel shows LCD2 and $j_{yv1,ext}$. Manual driving is represented by solid blue circles, automated driving A1 is black squares and A2 is grey diamonds.

TABLE VI
TIME GAP WITH RESPECT TO ADJACENT LEAD VEHICLE AT BI (CRITICAL B)

	$TG_{BI,alead}$ (s)				
Mode	Mean	Median	Std	Max	Min
Manual	1.1	1.0	0.3	1.8	0.8
Auto 1	2.4	2.3	0.1	2.7	2.2
Auto 2	2.3	2.3	0.1	2.4	2.2

a lane-change manoeuvre carried out on a straight road according to ISO 14791 [35]. However, the lane changes conducted in this paper are in general not carried out on a straight road and no correlation between duration and extremum of lateral acceleration can be found on an individual driver level. The lowest mean values of the extremum of lateral acceleration and jerk are found for the A1 approach and the highest for the A2 approach. In the right panel of Fig. 7, the relationship between the mean values of $j_{yv1,ext}$ and LCD2 indicate that a lower LCD2 implies a larger $j_{yv1,ext}$. The mean value of subject vehicle speed during the lane change for the manual drivers is 55 km h^{-1}, which is slightly lower than the mean values 63 km h^{-1} for the A1 and 64 km h^{-1} for the A2 approach.

2) Brake Manoeuvring (Critical B): Table VI shows the accepted safety margins for brake initiation, represented by statistics on $TG_{BI,alead}$. For manual driving, the mean value of the $TG_{BI,alead}$ is 1.1 s. For the automated approaches A1 and A2, the corresponding values are 2.4 and 2.3 s. In the bottom left panel of Fig. 8, the individual values of $\tau^{-1}_{max,alead}$ reveal that the braking situation for many drivers was moderately critical or non-critical ($\tau^{-1} \leq 0.2$). When the braking situation is non-critical, it is very hard to draw any conclusions regarding brake initiation triggered bottom-up by looming cues. It is plausible that braking initiation is stimulated by other visual cues, such as lead-vehicle brake-light onset. However, in the top panel of Fig. 8, the relationship between individual values of $\theta_{BI,alead}$ and $\dot{\theta}_{BI,alead}$, for the manual drivers, illustrated by solid blue circles, indicates a linear relationship ($R^2 = 0.82$, $p = .0004$). This suggests that information about the possibilities for action in a braking situation can be found in the optical flow variables. As mentioned above in Section II-B, brake initiation for automated approach A1 occurred when $TG_{BI,alead}$ was less than 2 s or $\dot{\theta}_{BI,alead}$ was less than 0.2° s^{-1}, respectively. This behaviour is indicated in the top panel of Fig. 8. For automated approach A2, there was no specific condition for brake initiation and the requested actuation was

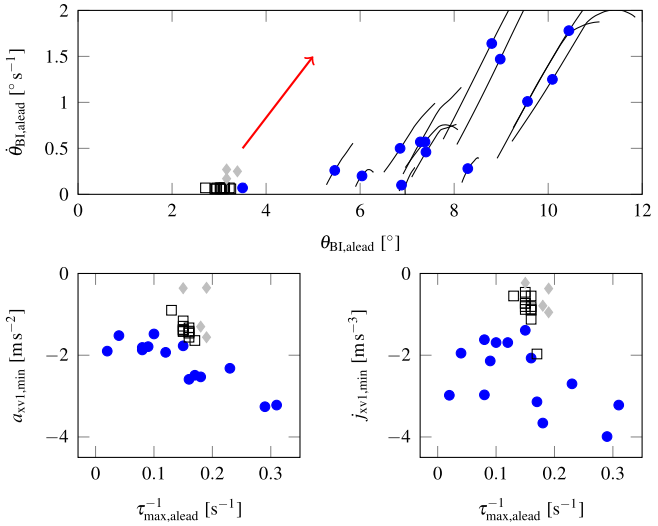

Fig. 8. Individual values for the critical B events. $\theta_{BI,alead}$ and $\dot{\theta}_{BI,alead}$ (top), $\tau^{-1}_{max,alead}$ and $a_{xv1,min}$ (bottom left) and $\tau^{-1}_{max,alead}$ and $j_{xv1,min}$ (bottom right). Manual driving is represented by solid blue circles. The solid black lines in the top right panel represents individual trajectories one second before and after BI. The red arrow indicate time course. Automated driving, are represented by black squares and grey diamonds for the A1 and A2 approaches.

a result of the optimisation formulation. For both automated driving approaches, brake initiation in general occurred earlier than in manual driving, and the brake initiation condition for the A1 approach was not supported by manual driving observations.

The bottom left panel of Fig. 8 illustrates individual values of $\tau^{-1}_{max,alead}$ and $a_{xv1,min}$. For manual driving the mean value of $\tau^{-1}_{max,alead}$ is 0.14 s^{-1}, while for automated approaches A1 and A2, the corresponding values are 0.15 and 0.18 s^{-1}. In all cases, brake execution was found to be safe. The maximum decelerations, characterising ride comfort, used in the brake executions were in general higher for manual than automated driving. The mean value of $a_{xv1,min}$ is -2.2 m s^{-2} for the manual drivers, while the corresponding values for the automated approaches A1 and A2 are -1.4 and -0.9 m s^{-2}. The higher deceleration in the manual driving is probably due to later brake initiation compared to automated driving. The manual drivers brake harder when $\tau^{-1}_{max,alead}$ increases ($R^2 = -0.88$, $p = .0001$). The same trend is also seen for the A1 approach. In the bottom right panel of Fig. 8, individual values of $j_{xv1,min}$ indicate that the jerk also increases when $\tau^{-1}_{max,lead}$ increases ($R^2 = -0.53$, $p = .005$).

3) Combined Braking and Steering (Critical A): As described in Section III-B, it was envisioned that the driver will either continue the lane change and combine braking and steering or abort the lane change by steering back to the initial lane and possibly braking. However, when inspecting video recordings of manual lane changes in the critical A event, it was noticed that the drivers' eye-movement behaviour during different phases before and during the lane change had a influence of how the vehicle was controlled. First, when the lane change was approaching, the drivers' visual focus shifted frequently between the current lane lead vehicle, adjacent lead vehicle and the rear-view mirror as the drivers were checking

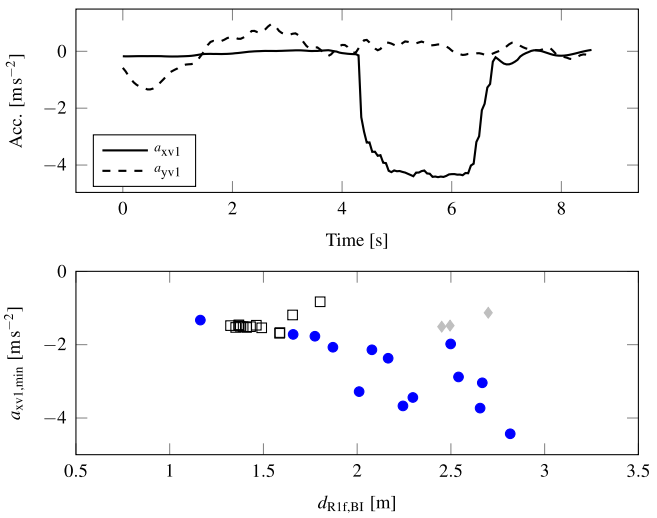

Fig. 9. Top panel: Example of typical utilised longitudinal and lateral acceleration for manual driving in the critical A event. Bottom panel: Individual values of $d_{R1f,BI}$ and $a_{xv1,min}$ for the critical A events. Manual driving is represented by solid blue circles. Automated driving, are represented by black squares and grey diamonds for the A1 and A2 approaches.

for a feasible gap to ensure safe manoeuvring. Second, in the first phase after the lane change was initialised, the drivers spent most of their visual focus looking in the rear-view mirror. This behaviour is most likely connected to the subject vehicle length and is probably different from passenger car driving. Third, once the front unit of the vehicle entered the target lane, the optical focus was redirected to the lead vehicle.

The drivers' eye-movement behaviour, combined with the event set-up, meant that steering and braking in general were separated. In the studied event, the adjacent lead vehicle started braking almost immediately after the lane-change initiation; see event design in Section II-C.3. In this situation, the drivers' optical focus was often directed towards the rear-view mirror and therefore the drivers often missed the brake onset of the adjacent lead vehicle. When the drivers shifted focus back towards the lead vehicles, the braking situation in many cases become relatively critical with a $\tau^{-1}_{max,alead} \geq 0.2$. None of the drivers tried to abort the lane change and steer back to the initial lane. In top panel of Fig. 9, utilised longitudinal and lateral acceleration of the first vehicle unit for one driver illustrates that the main part of the lane change for the first vehicle unit is completed at 4 s, when braking is initiated. Comparing the automated and manual driving during the critical A event, the automated driving performed simultaneous braking and steering control which was not the case for the manual drivers. The drivers' eye movement behaviour often led to late ($d_{R1f,BI} \geq 1.75$ m) and high ($a_{xv1,min} \leq -2$ m s^{-2}) deceleration levels, see bottom panel Fig.9. The mean value of the maximum deceleration for the manual drivers was decreased from -2.7 to -1.4 m s^{-2} in the automated driving case.

V. Conclusions

This paper presents a back-to-back performance comparison of lane-change manoeuvres, conducted in a driving simulator using an A-double long combination vehicle, applying two automated driving approaches and manual driving. The results from the automated driving approaches are very much dependent on the controller design and are difficult to generalize. However, studying the important actions and metrics of manual driving will give insight into how to design driving automation. The results provide evidence that both the time gap and relative speed to the adjacent lead vehicle are important for manual lane-change initiation. In addition, converting the time gap and relative speed into optical variables leads to similar indications of the possibility of safe lane-change initiation. The combination of time-gap and relative speed was not considered in the tested automated driving approaches.

The (non-critical) lane-change durations were considerably shorter for the automated driving approach based on optimisation than the manual driving. This behaviour also reflected higher mean values on lateral acceleration and jerk, which describe the level of ride comfort. All lane-change executions were found to be as safe including low levels of rearward amplification of lateral acceleration.

Brake initiation was studied using time gap and optical variables. Although, manual braking in general was considered to be moderately safety-critical, the results indicate that important information for brake initiation is reflected in optical variables. The threshold value for brake initiation used in the driver model based automated driving approach was not supported by manual driving observations.

The maximum decelerations used in the brake executions were in general higher for manual than automated driving. The maximum deceleration for the manual drivers correlates well with increased levels of the inverse of time-to-collision.

Combined braking and steering was investigated using a moderately safety-critical driving scenario. The driver's eye movement combined with the event set-up implied that steering and braking in general were separated in the case of manual driving. In the case of automated driving, steering and braking were combined and the mean value of the maximum deceleration was reduced compared to manual driving.

The result shows that the execution of manual driving can be well reflected with the lateral driver models as done in the A1 approach. Another option would be to tune the A2 approach by comparing the cost function components in (14) in the different driving scenarios and studying how the manual drivers prioritised the driving according to the cost function, then adjusting the weighting parameters accordingly, in order to make the A2 approach more human-like. Increased human-like behaviour can be important for operator acceptance of automated driving and for the surrounding traffic if a mixed population of manual and automated driving is a prerequisite. Additionally, it is likely that other highway scenarios e.g. managing dense traffic and/or a final distance to a target exit ramp, mandatory lane change, are fundamental for LCV usage and needs to be addressed.

References

[1] K. Bengler, K. Dietmayer, B. Farber, M. Maurer, C. Stiller, and H. Winner, "Three decades of driver assistance systems: Review and future perspectives," *IEEE Intell. Transp. Syst. Mag.*, vol. 6, no. 4, pp. 6–22, Winter 2014.

[2] E. Chan, "Overview of the sartre platooning project: Technology leadership brief," SAE Tech. Paper 2012-01-9019, 2012.

[3] A. Almevad. (2016). *Non Hit Car & Truck 2010-2015*. [Online]. Available: http://www.vinnova.se/sv/ffi/Back-up/Rapporter-fran-avslutade-projekt/Fordons—trafiksakerhet/

[4] AdaptIVe. (2016). *European Commision CORDIS, FP7-ICT, 610428*. [Online]. Available: http://cordis.europa.eu/project/rcn/191624_en.html

[5] C. Nowakowski, S. E. Shladover, and H.-S. Tan, "Heavy vehicle automation: Human factors lessons learned," *Procedia Manuf.*, vol. 3, pp. 2945–2952, 2015. [Online]. Avaialbe: http://www.sciencedirect.com/science/article/pii/S2351978915008252

[6] SAE International, "SAE J2944 Operational Definitions of Driving Performance Measures and Statistics," SAE Tech. Peper. J3016, 2015.

[7] J. Aurell and T. Wadman, "Vehicle combinations based on the modular concept," Nordic Road Association, Linköping, Sweden, NVF, Tech. Rep. 1, 2007.

[8] Vinnova 2011-04411. (2016). *Säkra Korridorer, Höghastighetsreglering av Långa Fordonskombinationer*. [Online]. Available: http://www.vinnova.se/sv/Resultat/Projekt/Effekta/2009-02186/Sakra-korridorer-hoghastighetsreglering-av-langa-fordonskombinationer/

[9] P. Nilsson, L. Laine, B. Jacobson, and N. Van Duijkeren, "Driver model based automated driving of long vehicle combinations in emulated highway traffic," in *Proc. IEEE 18th Int. Conf. Intell. Transp. Syst. (ITSC)*, Sep. 2015, pp. 361–368.

[10] N. van Duijkeren, T. Keviczky, P. Nilsson, and L. Laine, "Real-time NMPC for semi-automated highway driving of long heavy vehicle combinations," *IFAC-PapersOnLine*, vol. 48, no. 23, pp. 39–46, 2015.

[11] P. Nilsson, L. Laine, N. van Duijkeren, and B. Jacobson, "Automated highway lane changes of long vehicle combinations: A specific comparison between driver model based control and non-linear model predictive control," in *Proc. Int. Symp. Innov. Intell. Syst. Appl. (INISTA)*, Sep. 2015, pp. 1–8.

[12] V. Punzo and B. Ciuffo, "Integration of driving and traffic simulation: Issues and first solutions," *IEEE Trans. Intell. Transp. Syst.*, vol. 12, no. 2, pp. 354–363, Jun. 2011.

[13] M. Aeberhard *et al.*, "Experience, results and lessons learned from automated driving on Germany's highways," *IEEE Intell. Transp. Syst. Mag.*, vol. 7, no. 1, pp. 42–57, Spring 2015, doi: 10.1109/MITS.2014.2360306.

[14] Daimler AG. (2016). *Pioneering Achievement: Autonomous Long-Distance Drive in Rural and Urban Traffic—Mercedes-Benz S-Class Intelligent Drive Drives Autonomously in the Tracks of Bertha Benz*. [Online]. Available: http://media.daimler.com

[15] D. N. Lee, "A theory of visual control of braking based on information about time-to-collision," *Perception*, vol. 5, no. 4, pp. 437–459, 1976.

[16] B. R. Fajen, "Perceiving possibilities for action: On the necessity of calibration and perceptual learning for the visual guidance of action," *Perception-London*, vol. 34, no. 6, pp. 717–740, 2005.

[17] P. G. Gipps, "A model for the structure of lane-changing decisions," *Transp. Res. B, Methodol.*, vol. 20, no. 5, pp. 403–414, Oct. 1986.

[18] P. Hidas, "Modelling lane changing and merging in microscopic traffic simulation," *Transp. Res. C, Emerg. Technol.*, vol. 10, nos. 5–6, pp. 351–371, Oct./Dec. 2002.

[19] A. Kanaris, E. B. Kosmatopoulos, and P. A. Loannou, "Strategies and spacing requirements for lane changing and merging in automated highway systems," *IEEE Trans. Veh. Technol.*, vol. 50, no. 6, pp. 1568–1581, Nov. 2001.

[20] W. van Winsum, D. de Waard, and K. A. Brookhuis, "Lane change manoeuvres and safety margins," *Transp. Res. F, Traffic Psychol. Behaviour*, vol. 2, no. 3, pp. 139–149, Sep. 1999.

[21] M. F. Land and D. N. Lee, "Where we look when we steer," *Nature*, vol. 369, pp. 742–744, Jun. 1994.

[22] D. D. Salvucci and A. Liu, "The time course of a lane change: Driver control and eye-movement behavior," *Transp. Res. F, Traffic Psychol. Behaviour*, vol. 5, no. 2, pp. 123–132, Jun. 2002.

[23] D. D. Salvucci and R. Gray, "A two-point visual control model of steering," *Perception*, vol. 33, no. 10, pp. 1233–1248, 2004.

[24] J. M. Flach, M. R. Smith, T. Stanard, and S. M. Dittman, "Collisions: Getting them under control," *Adv. Psychol.*, vol. 135, pp. 67–91, 2004.

[25] R. J. Kiefer, D. J. LeBlanc, and C. A. Flannagan, "Developing an inverse time-to-collision crash alert timing approach based on drivers' last-second braking and steering judgments," *Accident Anal. Prevention*, vol. 37, no. 2, pp. 295–303, Mar. 2005.

[26] M. R. Smith, J. M. Flach, S. M. Dittman, and T. Stanard, "Monocular optical constraints on collision control," *J. Experim. Psychol., Human Perception Perform.*, vol. 27, no. 2, p. 395, 2001.

[27] H. Sun and B. J. Frost, "Computation of different optical variables of looming objects in pigeon nucleus rotundus neurons," *Nature Neurosci.*, vol. 1, no. 4, pp. 296–303, 1998.

[28] L. Laine, "Reconfigurable motion control systems for over-actuated road vehicles," Ph.D. dissertation, Dept. Appl. Mech., Chalmers Univ. Technol., Gothenburg, Sweden, 2007.

[29] K. Tagesson, P. Sundström, L. Laine, and N. Dela, "Real-time performance of control allocation for actuator coordination in heavy vehicles," in *Proc. IEEE Intell. Vehicles Symp.*, Jun. 2009, pp. 685–690.

[30] P. Nilsson and K. Tagesson, "Single-track models of an A-double heavy vehicle combination," Chalmers Univ. Technol., Gothenburg, Sweden, Tech. Rep. 8, 2013.

[31] J. Jansson, J. Sandin, B. Augusto, M. Fischer, B. Blissing, and L. Källgren, "Design and performance of the VTI Sim IV," in *Proc. Driving Simulation Conf.*, Paris, France, Sep. 2014, pp. 1–4.

[32] B. Augusto, P. Nilsson, L. Laine, J. Sandin, and N. Fröjd, "Using large moving base simulators as tool when designing future automated functionality for commercial heavy vehicles: A case study of highway auto-piloting for high capacity transport," presented at 14th Int. Symp. Heavy Vehicle Transp. Technol. (HVTT14), New Zealand, 2016.

[33] A. Nåbo, C. Andhill, B. Blissing, M. Hjort, and L. Källgren. (2016). *Known Roads—Real Roads in Simulated Environments for the Virtual Testing of New Vehicle Systems*. [Online]. Available: http://www.vipsimulation.se/?page=vip-reports&pid=254

[34] SAE International, "SAE J3016 Taxonomy and definitions for terms related to on-road automated motor vehicles," SAE Tech. Paper J2944, 2014.

[35] *Road Vehicles—Heavy Commercial Vehicle Combinations Articulated Buses—Lateral Stability Test Methods*, ISO Standard 14791:2000, 2010.

Peter Nilsson received the M.Sc. degree in mechanical engineering from Chalmers University of Technology, Gothenburg, Sweden, in 2000, where he is currently working toward the Ph.D. degree with the Department of Applied Mechanics. Since 2000, he has been with the Volvo Group Trucks Technology, Gothenburg. From 2002 to 2012, he was a Senior Vehicle Analyst in vehicle dynamics and noise and vibration isolation.

Leo Laine received the Ph.D. degree from Chalmers University of Technology, Gothenburg, Sweden, within the topic of Hybrid Electric Vehicles illustrating how vehicle stability control is balanced with energy management for over-actuated vehicles. Since 2007, he has been with the Volvo Group Trucks Technology in Chassis as a Senior Technology Specialist within complete powertrain and vehicle control. Since 2013, he has also been an Adjunct Professor in vehicle dynamics with Chalmers Vehicle Engineering and Autonomous Systems.

Bengt Jacobson received the Ph.D. degree in machine elements from Chalmers University of Technology, Gothenburg, Sweden, in 1993. He was a Technical Expert with Volvo Car Corporation, Gothenburg, from 2001 to 2010, with a focus on vehicle dynamics control and active safety. He is currently a Professor of Vehicle Dynamics with the Department of Applied Mechanics, Chalmers University of Technology.